GLOBAL BIOGEOCHEMICAL CYCLES, VOL. 7, NO. 1, PAGES 229-244, MARCH 1993

IRON FERTILIZATION OF THE AUSTRAL OCEAN - THE HAMBURG MODEL ASSESSMENT

Katharina D. Kurz and Ernst Maier-Reimer

Max-Planck-Institut für Meteorologie, Hamburg, Germany

Abstract. We have investigated the effect of an enhanced biological productivity, caused by an artificial iron fertilization, in the southern ocean with a three-dimensional carbon cycle model, which is based on an ocean circulation obtained by an ocean general circulation model. The increase of the biological production did not result in a substantial increase of CO_2 uptake by the ocean, as it has been proposed by Martin et al. (1990). We have found that - assuming that the basic structure of the particulate downward flux does not change when higher production occurs - the ocean circulation provides a higher return flux of remineralized products that compensates two thirds of the effect of the higher export production on the atmospheric pCO_2. This finding is only slightly modified when assuming a much deeper penetration of particle flux due to the fertilization. Owing to the nonlinearity of the buffer factor the absolute value of CO_2 reduction in the atmosphere is higher at high levels of pCO_2. In view of the logarithmic dependency of the radiative forcing on CO_2, the fertilization is more efficient at low CO_2 levels. With our carbon cycle model we have, in essence, confirmed earlier three-dimensional model studies with a simplified geochemical cycling of the Princeton group (Sarmiento and Orr, 1991).

Paper number 92GB02910.
0886-6236/93/92GB-02910$10.00

INTRODUCTION

The increase of CO_2 in the atmosphere with the expected climate change has stimulated a widespread search for technical solutions to reduce the atmospheric CO_2 level. One proposal was made by Martin et al. [1990], who had found that the biological growth rate is limited by the lack of iron in the Southern Ocean; thus an artificial iron fertilization would increase biological production and therefore decrease substantially the atmospheric carbon content.

The total inventory of phosphate in the ocean would be equivalent to the incorporation of 4000 Gt C into organic material, if no remineralization would occur. For a quantitative assessment of the fertilization effectiveness, a naive assumption of this large number would be, however, rather misleading. The atmospheric pCO_2 is controlled by the chemistry of the surface ocean. The annual mean global average phosphate concentration in the surface ocean is now at

0.58 μmol L^{-1}. A complete removal of the surface phosphate by enhanced biological activity would reduce the surface concentration of dissolved inorganic carbon by 70μmol L^{-1}, or 3.7% of the typical values. The corresponding reduction of the atmospheric pCO_2 by 37% (assuming an average buffer factor of 10 for the present days ocean) or 220 Gt C has to be considered as an upper limit for the potential effects of the fertilization.

A lower estimate of the possible impact of iron fertilization in the southern ocean is given by Davies [1990]. He has pointed out that with the incorporation of all available nutrients in the austral surface water into organic material the anthropogenic carbon emission of only one year could be additionally stored in the ocean.

The effective storage of CO_2 evolves from the new equilibrium between the enhanced supply of the surface waters with remineralized nutrients (and associated additional CO_2) and the long-term deep transport of organic material out of the region of the fertilization.

Box model studies [Peng and Broecker, 1991a, b; Joos et al., 1991] show indeed that details in the parametrization of the ocean circulation have a strong impact on the efficiency of the proposed iron fertilization.

A shortcoming of box models is that the flow field is obtained by fitting the model to tracer distributions, traditionally radiocarbon either natural or bomb produced. It has been demonstrated that the answer of the model [Siegenthaler, 1983] will depend not only on the layout of the model but also on the principal tracer of the calibration. Thus it appears essential to treat the ocean circulation as realistic as possible.

Sarmiento and Orr [1991] recently presented a study where iron fertilization was applied as a perturbation to the model by Najjar et al. [1992]. In this model, the basic state is achieved by restoring the surface concentration of phosphate in regions where the model tends to predict higher than observed PO_4 concentration. The difference is interpreted as export production and redistributed over depths. Around Antarctica, the resulting values indicate an unrealistically high production. Here, obviously, the circulation field of the model is not fully consistent with the data of PO_4. The gross structures of the deep distribution of phosphate, however, are simulated realistically.

For the evaluation of the iron fertilization, they accordingly set the surface values of PO_4 south of 30°S to zero. The changes of the PO_4 distribution are then transformed by means of the Redfield ratio and buffer factor into atmospheric pCO_2. In their model, the effectivity of the iron fertilization is in the range of the Peng and Broecker [1991a, b] experiments but definitely lower than in the Joos et al. [1991] model.

In this paper we describe a series of experiments that we have performed with the global three-dimensional Hamburg carbon cycle model [Maier-Reimer and Bacastow, 1990; Heinze et al., 1991]. The oceanic circulation fields are provided by the large-scale geostrophic (LSG) ocean model [Maier-Reimer et al., 1993] and agree essentially with observation of global water mass transport and deep water formation. On the basis of this more realistic representation of ocean dynamics, we estimate the impact on the global carbon cycle if the biological productivity of the southern ocean is artificially increased. An introduction of the basic structure of the model and its steady state is followed by a description of the experiments and their results. We test the sensitivity of our results to a change in the vertical mixing and in the structure of the downward flux of particles. Our findings are compared to results of box model studies [Peng and Broecker, 1991a, b; Joos et al., 1991] and the three-dimensional perturbation model of Sarmiento and Orr [1991].

MODEL

Our carbon cycle model is based on the circulation field provided by an ocean general circulation model (OGCM) which is forced with realistic wind fields [Hellermann and Rosenstein, 1983] and relaxed toward surface boundary conditions [Levitus, 1982; Woodruff et al., 1987]. In that configura-

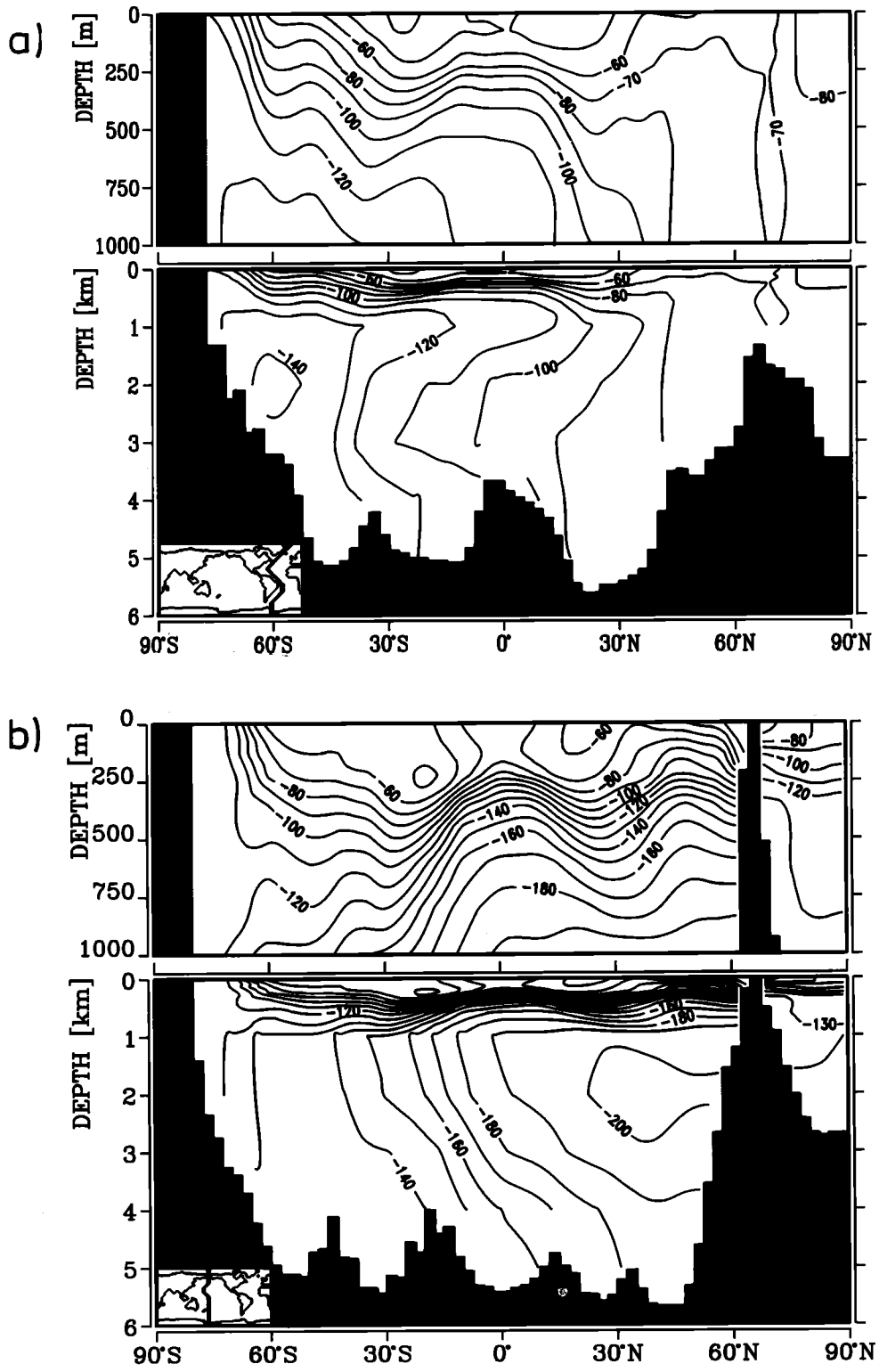

Fig. 1. Model distribution of natural (i.e., preindustrial) radiocarbon (in ‰) in the (a) Atlantic and the (b) Pacific along Geosecs sections as indicated by the map in the lower left corner. In the upper panel the upper kilometer is again displayed with higher resolution.

tion, we had little chance to tune systematically any parameter. From a series of five experiments with different plausible thermohaline forcing we choose the one that gave the most realistic reproduction of the GEOSECS Atlantic radiocarbon [Stuiver and Östlund, 1980]. A detailed discussion is given by Maier-Reimer et al. [1993]. The model thus can be understood as tuned to natural radiocarbon. The distribution of natural radiocarbon in the OGCM's steady state, drawn along GEOSECS section (Figure 1) , shows realistic gradients in the deep ocean; around Antarctica, however, the values are too high (-130 ‰ instead of -160 ‰). Consequently, the radiocarbon values of the water in the Northern Pacific are also higher than observed (+30 ‰). This misfit can be attributed to a too strong vertical mixing in that region, but also to an overestimate of the air to sea gas exchange. With the wind field analyses of European Center for Medium Range Weather Forecasts and the parametrization by Liss and Merlivat [1986], Heimann and Monfray [1989] have constructed a global map of gas exchange coefficients with a global average of 0.039 mol m^{-2} yr^{-1} ppm^{-1}. We have normalized these fields to the global average value of 0.06 mol m^{-2} yr^{-1} ppm^{-1}, as derived from the inventory of bomb produced radiocarbon [Broecker et al., 1985].

On the basis of the physical fields from the OGCM the carbon cycle model calculates the distribution of and interaction between inorganic and organic carbon in the ocean including carbon transfer across the air-sea interface and burial in sediments. The time step of 1 month is the same as in the physical part. In contrast to the physical model, where surface values of temperature and salinity are restored to climatological distributions the geochemical model has no restoring terms except for the surface oxygen concentration which is set to the local saturation value. All gradients of the model are created by the internal dynamics. With given inventory of PO_4 and alkalinity, only the inventory of ΣCO_2 was tuned to yield a realistic value for atmospheric pCO_2 concentration at a preindustrial level of approximately 280 ppm (see Table 1).

The biological fixation of carbon is controlled by a production scheme based on the phosphate concentration (we use phosphate as the limiting nutrient to avoid problems with the representation of the denitrification processes) and a growth function depending mainly on light, temperature, and turbulence conditions. We are interested only in that part of the gross production that is sinking out of the euphotic zone, which is represented in the model by the uppermost layer and has a globally uniform thickness of 50 m. This "export" production E is written as

$$E = r_0 P cos\Delta \frac{50\,m}{C_d} \frac{(T+2)}{(T+10)} \frac{P}{(P+P_0)} \quad (1)$$

where P is the local phosphate concentration, Δ is the solar angle, C_d is the depth of convection in meter and T is the surface tem-

TABLE 1. Pool Size and Mean Concentration of Different Tracer in the Hamburg Carbon Cycle Model

	Pool Size		Mean Concentration	
Carbon dioxide in atmosphere	600	Gt C	281	ppm
Total inorganic carbon in the ocean	37150	Gt C	2180	μmol C L^{-1}
Organic carbon in the ocean	110	Gt C		
Calcium carbonate in sediment	4570	Gt C		
Organic carbon in sediment	4	Gt C		
Alkalinity	3287	10^{15} equiv.	2315	μequiv. L^{-1}
Phosphate	2.9	10^{15} mol	2.05	μmol L^{-1}
Silicate	169	10^{15} mol	119	μmol L^{-1}
Oxygen	294	10^{15} mol	207	μmol L^{-1}

perature in degrees Celsius. The last term on the right-hand side of the equation describes the reduction of productivity at low nutrients (Michaelis-Menten kinetics) where P_0 is the half saturation constant. We set $P_0 = 0.02$ μmolP L^{-1} which is equivalent to the half saturation values for nitrate given by Eppley et al. [1969] for oceanic species when scaled with the Redfield ratio P:N = 1:17. r_0 equals 1/4 month^{-1} and has been tuned to yield realistic surface phosphate concentrations.

The annual mean phosphate concentration (Figure 2a) is in reasonable agreement with the data by J. R. Reid (personal communication, 1990; Figure 2b). The high phosphate concentration at the surface around Antarctica is maintained in the model by the reduction of the productivity due to low temperature (annual mean temperature effect : 0.3, see equation (1)) and high rates of convective overturning (annual mean convection effect : 0.2, see equation (1)). Additional light conditions are poor during 6 months of the year.

The export of phosphate is linked with an export of carbon in a constant Redfield ratio. On the basis of this formulation the global annual export production in the steady state model is 8.5 Gt C yr^{-1}. Its structure, shown in Figure 3, is determined primarily by the Ekman dynamics of the physical model. We

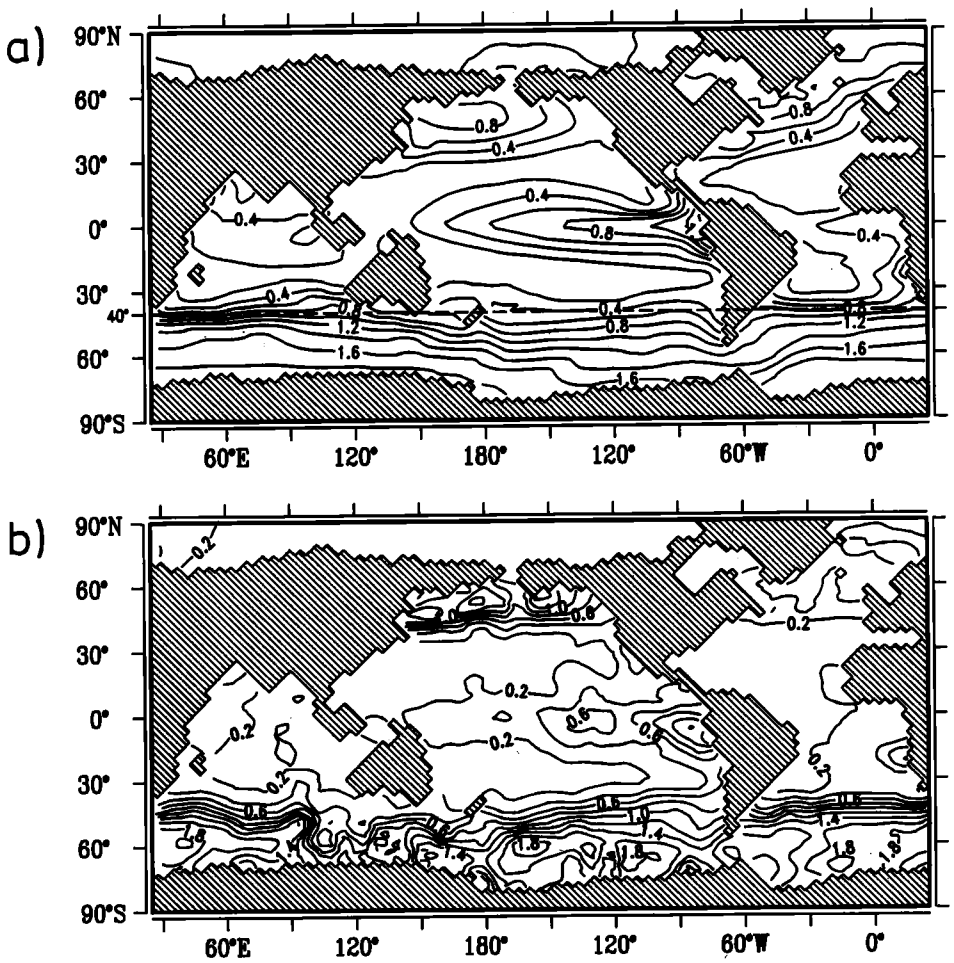

Fig. 2. Surface distribution of phosphate (in μmol L^{-1}) (a) Model results, (b) data by J. Reid (personal communication, 1990). The dashed line in Figure 2a indicates the northern border of the fertilization region.

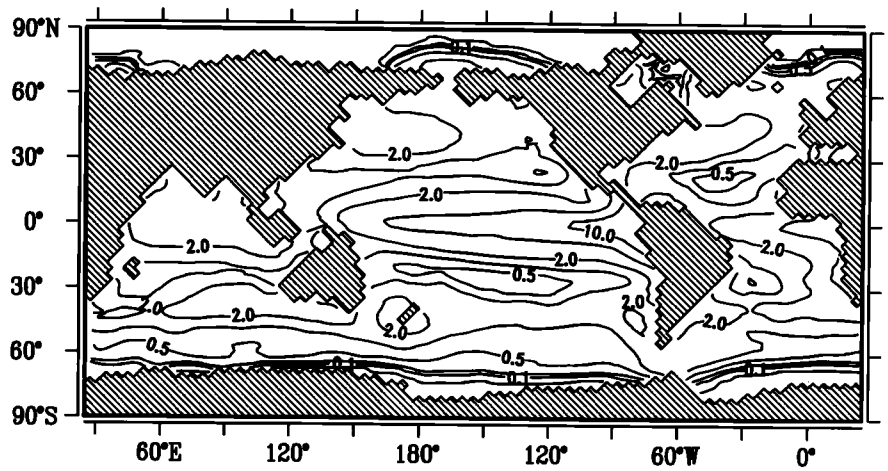

Fig. 3. Annual mean production of organic material in logarithmic contour intervals 0.1, 0.2, 0.5, 1., 2., 5., 10., 20. g m^{-2} $month^{-1}$.

note the absence of the high production regions of continental shelves, which are not resolved in our model. The highest production is in the eastern equatorial Pacific due to the strong upwelling. The production in the area of the proposed iron fertilization is low (1.3 GtC yr^{-1}) due to cumulative limitation effects of the production factor.

The composition of the organic matter is based on the Redfield ratios

$$P : N : C : \Delta O_2 = 1 : 17 : 122 : -175$$

where ΔO_2 denotes the oxygen exchange with the surrounding water. Nitrate is considered only for a correction of the alkalinity changes during biological production and remineralization.

In addition to the incorporation of carbon into soft tissue, which decreases the partial pressure, calcite shell producers incorporated carbonate and change therefore the total inorganic carbon concentration and the alkalinity in a way which increases the carbon dioxide partial pressure. The production of calcite shells in the model is mainly governed by the production of soft tissue, modified by the available silicate concentration and the local temperature. We assume that in cold and silicate rich water, the formation of diatoms and radiolarians is preferred. The resulting calcite production is higher in the Atlantic where low silicate concentrations are predicted.

The global average ratio of soft tissue to hard part production in the model is about 5:1 which is slightly higher than the value 4:1, derived from typical surface to depth differences of alkalinity and Σ CO_2 [Broecker and Peng, 1982].

The newly produced particulate organic material (POC) is distributed over depth z according $(z/100\ m)^{-0.8}$ for $z > 100$ m, as deduced from sediment traps data [Suess, 1980; Berger et al., 1987]. With this structure of the flux we simulate a realistic position of phosphate maximum and oxygen minimum at the depth of 0.5 - 1 km. It has been speculated [Martin, 1990] that in high latitudes the particle flux should reach much deeper, involving remineralization primarily at the seafloor. We feel, however, that the existence of a pronounced phosphate maximum at 500 m even at 60°S [cf. Bainbridge, 1981] contradicts this idea.

POC is advected by the general circulation as a passive tracer and remineralizes with a time constant of 4 years, if oxygen is available. At O_2 levels below 10 μmol L^{-1}, remineralization is blocked. We have chosen this treatment of POC, without too much geochemical interpretation, to avoid negative oxygen concentrations. High concentrations of POC indicate regions where denitrification or sulfate reduction - not treated by the model - should occur. The model is stationary with a pool of 110 Gt of carbon in form

of POC, most of it being found in the eastern subequatorial Pacific. The size of this pool indicates that the equatorial production is strongly overestimated by the model. This could be due to an overestimate of the physical upwelling from the prescribed wind field. In the real ocean, however, the production could also be reduced again due to the lack of iron in that region. We note that in Najjar's standard experiment phosphate concentrations of up to 5 μmol kg^{-1} are predicted here, which corresponds to the sum of dissolved and organically fixed phosphate in our model. Both models react, apparently, very similarly to the prescribed wind field.

The hard parts are distributed with exponential profiles. The removal of silicate from the surface is more efficient than for phosphate [cf. Bainbridge, 1981]. This is modeled by the assumption of a much greater penetration (4 km e-folding depth). The released opal is dissolved instantaneously. Figure 4a and 4b show the resulting distributions for phosphate and silicate along a section in the western Atlantic. The relation between Antarctic and North Atlantic deepwater concentrations is 1.5 for phosphate and 6 for silicate.

For calcium carbonate we take a penetration depth of 2 km. The dissolution of calcium carbonate depends on the local degree of supersaturation with respect to calcite. The resulting depth of the lysocline is at 1 km in the Northern Pacific and over 4 km in the Northern Atlantic (E. Maier-Reimer, Geochemical cycles in an ocean general circulation model, 1, Tracer distribution, submitted to Global Biogeochemical Cycles, 1993).

EXPERIMENT

The purpose of our study is to assess the impact of an enhanced productivity in the southern ocean on the global carbon cycle. The biological production in the model is a function of the nutrient concentration and a basic growth parameter which is modified by light, temperature, turbulence, and sea ice conditions. Around Antarctica, the limitations reduce the productivity. In the experiments described below, we assume that the proposed iron fertilization [Martin et al., 1990] could increase the productivity and overcome all other limitations; i.e., we prescribe the production as a function of nutrients only. We restrict, however, the effects of fertilization to the months October to March. The rest of the year the limiting conditions are too severe to support biological production. The only limitation during the southern summer months is the presence of a persistent ice cover near the coast of Antarctica. It is always assumed in the model that there is no biological production below sea ice.

The artificial enhancement of the biological productivity is restricted to the region south of 40°S. This area covers about 55 million square kilometers, i.e., 15% of the global ocean surface. The mean surface phosphate concentration in this area is 1.35 μmolP L^{-1} for the reference experiment.

For a better discrimination between the partly opposing effects of the various processes involved, we test the impact of iron fertilization on the anthropogenically undisturbed modes starting the integration from a preindustrial steady state. Additionally, we performed fertilization experiments and the corresponding control experiments without fertilization for two scenarios with anthropogenic CO_2 emissions: a "business-as-usual" scenario with an increase in fossil fuel emission according to the estimates of Intergovernmental Panel on Climate Change (IPCC) [Houghton et al., 1990] with a linear interpolation between the numbers given for selected years and a second scenario with a constant emission rate of 6.15 Gt C yr^{-1}. The starting distributions are obtained by integration of the model from the steady state (1800) to the end of 1989 assuming an anthropogenic CO_2 emission after Boden et al. [1992]. Additionally there is a source of CO_2 from the terrestrial biosphere after Peng et al. [1983] scaled to a maximum of 0.6 GtC yr^{-1} at the turn of the century and extrapolated until 1990. In 1990 it is assumed that 0.2 GtC yr^{-1} are released by the biosphere. We note that with this forcing, the increase of atmospheric CO_2 is overestimated as compared to observations (376 ppm instead of 353 ppm in 1990) [Houghton et al., 1990].

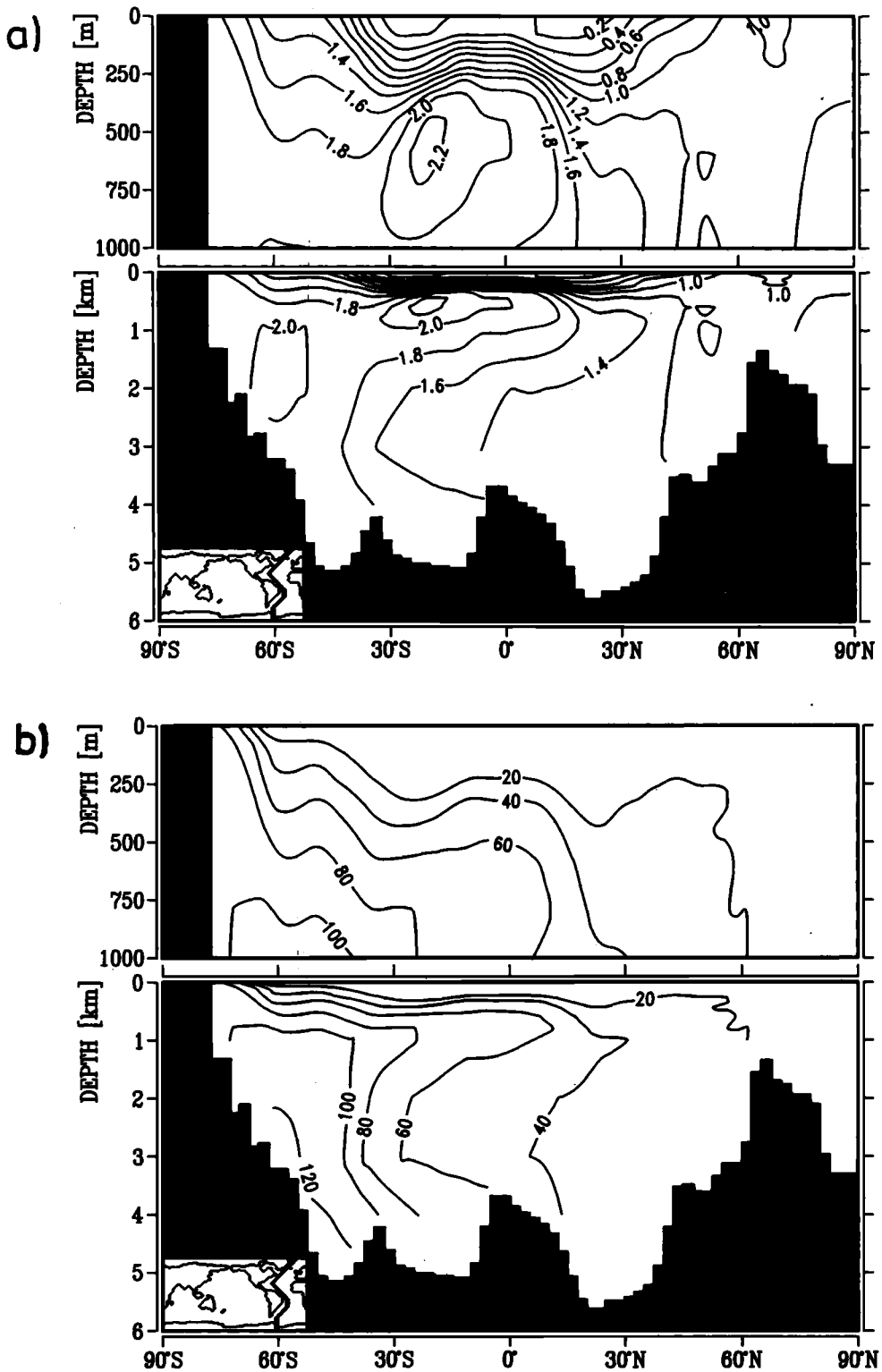

Fig. 4. Model distributions in the control run along the Geosecs section in the Western Atlantic: (a) phosphate (in μmol L^{-1}) and (b) silicate (in μmol L^{-1}). In the upper panel the upper kilometer is again displayed with higher resolution.

This discrepancy may be explained partly from the structure of the models main thermocline, which is too shallow; the role of the terrestrial biosphere, on the other hand, is still controversary (Houghton et al., [1990] versus Tans et al. [1990]). When forcing the model with prescribed atmospheric concentrations [Siegenthaler and Oeschger, 1987; Boden et al., 1992], the model ocean takes up 1.54 Gt of carbon in 1988, implying that there should be another sink (not necessarily the terrestrial biosphere) of about 0.7 GtC yr^{-1}. The corresponding numbers for the Princeton model [Sarmiento et al., 1992] whose thermocline is twice as deep as ours, are 1.9 and 0.3 GtC yr^{-1}, respectively. Both numbers for the unexplained sink are definitely less than the Tans et al. estimate for the sink in northern hemisphere continents. For the experiments described below, we preferred to keep the input function continuous; i.e., we started with the unrealistic high value of 376 ppm in 1990.

RESULTS

Fertilization Without CO_2 Emissions

The enhanced biological production reduces the atmospheric CO_2 level by 34 ppm after 100 years which corresponds to a net storage of 73 Gt C in the ocean. This effect is composed of different processes, involving the budgets of phosphate and alkalinity and the air to sea gas transfer.

The iron fertilization increases the productivity south of 40°S and thus leads to a different vertical distribution of nutrients. After an initial peak where nearly all nutrients in the region of fertilization are removed from the surface layer, a new balance establishes between the increased downward flux of nutrients incorporated into organic matter and the upward transport of remineralized nutrients by advection. The global annual export production increases by 2.2 GtC yr^{-1}, as compared to the control run. In the region of fertilization the export production is enhanced by 2.8 GtC yr^{-1} while in the adjacent parts of the ocean the export production decreases by 0.6 GtC yr^{-1}. This is due to a shift of the production zone, which is now more closely confined to the upwelling region. Figure 5 displays the zonally integrated meridional stream function in the upper kilometer together with the relase of POC in the fertilization experiment. The high productivity leads to the consumption of nearly all nutrients as soon as they appear in the euphotic layer (during the months October to March), while in the control run, unused phosphate reaches the downwelling areas around 30°S where the circulation supports the removal of the produced organic material from the surface region. The change of the magni-

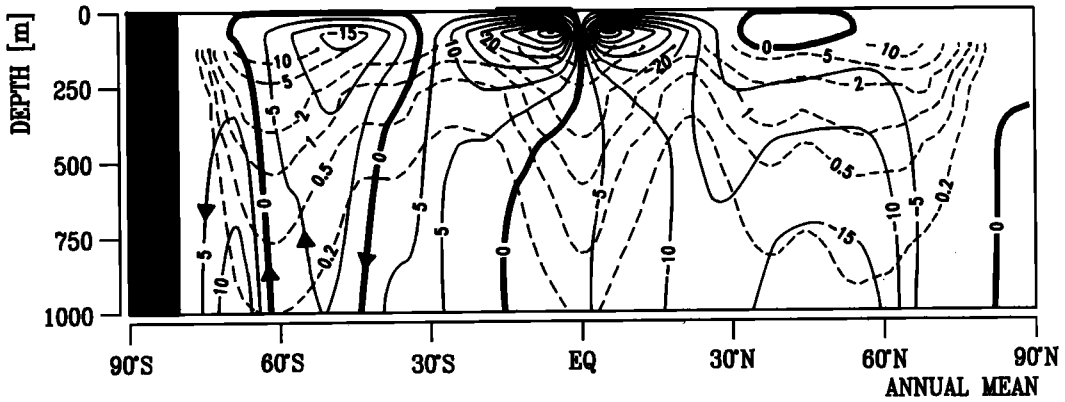

Fig. 5. Zonal mean streamfunction (solid lines, in Sv=10^6 m^3 s^{-1}, contour interval 5 Sv) and annual release of organic matter from surface layer production (dashed lines, Contours are drawn at 0.1, 0.2, 0.5, 1., 2., 5., 10. μmol C L^{-1} yr^{-1}).

tude leads to an increased flux out of the euphotic zone, but the focussing on the upwelling area feeds an enhanced recirculation of organic matter.

A simple advection experiment serves to identify the role of mixing and upwelling for the redistribution of nutrients to the surface: We introduce an artificial tracer which is set initially to zero except in the region of fertilization. Here we distribute Reid's surface phosphate data over depth according to our penetration profile for POC. During the integration, the surface values of this tracer are set to zero. The decay of the inventrory then gives a direct measure for the involved time constants. 15% are lost within the first year, while after ten years the pool has been reduced to 47% of its initial value. At the end of the 100 years integration, the remaining 21% are distributed over large parts of the southern deep ocean. This behaviour explains that the long term storage is less than half of the cumulative additional production in the fertilization scenario.

As nutrients are displaced to greater depths, also carbon is transported and stored at deeper layers. The global mean phosphate concentration in the upper water column decreases by 0.4 μmolP L^{-1} within 100 years of fertilization. The total amount of phosphate reduction in the corresponding volume is equivalent to 49 Gt of carbon (=23 ppm) assuming the Redfield ratio C:P of 122:1. 67% of the computed uptake (73 Gt C) can thus be explained by the redistribution of nutrients.

The remaining fraction of the additional uptake of CO_2 originates in our model from the nature of the organisms that are produced. The model distinguishes between opal producers (diatoms, radiolarian, etc.) and calcite producers (coccolithophores, foraminifera, etc.). Organisms that use silicate of their shells change the total amount of dissolved inorganic carbon (ΣCO_2) and alkalinity according to their content of soft tissue, which yields a lower partial pressure (pCO_2). A strong diatom bloom can lead to a pCO_2 reduction of up to 200 ppm [Whitfield, 1991]. However, the effect on the pCO_2 is diminished if the ΣCO_2 reduction is accompanied by an alkalinity reduction, as in the case of coccolithophores production.

In the fertilization run the global export production is shifted towards the cold regions closely confined to the Antarctic divergence zone, where the low temperatures inhibit the formation of calcite. In the adjacent subtropical regions, where the warm temperatures support the formation of calcite shells, the overall production decreases and yields, thus a reduction of the alkalinity export. The global averaged C_{org}:C_{CaCO_3} rain ratio changes accordingly from 5:1 to approximately 8:1 and the surface alkalinity increases by up to 12 μequiv. L^{-1}.

This mean gain of 0.5% alkalinity in the surface water decreases the partial pressure by 15.1 ppm in surface water.

The apparent discrepancy between the computed uptake of 73 Gt (= 34 ppm) after 100 years and the sum of the two potentials (23 ppm+15 ppm) at this still transient state may be explained by the slowness of the air-sea gas exchange. We assume in the fertilization complete removal of nutrients from the surface within one month, whereas the gas exchange operates with a time constant of approximately 5 months for a 50-m surface layer. This is consistent with results of Sarmiento et al. [1992], who have indeed pointed out that a doubling of the gas exchange coefficient increases the uptake of CO_2 by 10%.

The existence of the air-sea gas exchange also influences the evolution of the system to reach a new equilibrium. Figure 6 displays the time evolution of the global net fluxes of total CO_2 and phosphate in its carbon equivalent (both including the contribution from POC) across the 100-m depth horizon. Phosphate and particle fluxes equilibrate almost perfectly within the first decade while the CO_2 equilibrates rather on a centennial time scale, which is the familiar time scale from studies on the oceanic CO_2 uptake of fossil fuel emissions.

Because of the additional transport path via the atmosphere the carbon cycle can develop a closed global path through the

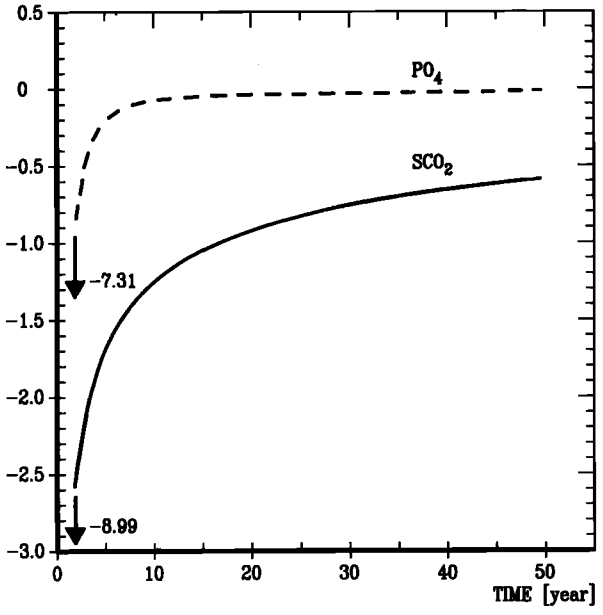

Fig. 6. Time series of the globally integrated effective removal from the upper 100 m of dissolved inorganic carbon (SCO_2) and carbon equivalent - according to the Redfield ratio - phosphate (PO_4) (in Gt C yr^{-1}). Negative values for phosphate indicate a depletion of the surface inventory. Since the ocean is an open system for carbon dioxide, the amplitude of the imbalance potentially equals the CO_2 - uptake from the atmosphere. The value -8.99 (-7.31) Gt C corresponds to the imbalance in the first year for SCO_2 (PO_4), where due to fertilization the phosphate concentration in the austral ocean is strongly depleted.

deep ocean and the atmosphere whose effective time constant is determined by the long flushing time of the deep ocean, while for phosphate, the deep ocean acts as a relatively inert reservoir and the effective time constants are stronger determined by surface processes.

Impacts on oxygen

It was pointed out by Joos et al. [1991] that a higher productivity could lead to anoxic conditions in the ocean. This conjecture is partly confirmed by our experiment: in the deep Pacific, the oxygen concentration is reduced by 10 to 30 μmol L^{-1} (Figure 7). A peculiar increase of the subsurface oxygen content is found near 20°S. The shift of the production zone towards Antarctica reduces the production in the adjacent downwelling regions, so that less organic matter is released. The consumption of oxygen due to remineralization processes is then reduced, too.

Sarmiento and Orr have simulated a similar structure of oxygen variations due to the fertilization but with a twice as high amplitude. The difference in the predicted oxygen consumption after 100 years of simulation may be partly attributed to the deeper penetration of organic material in their model. This provides a stronger separation of the locations of oxygen production and oxygen depletion than in our model. A more important contribution comes from the simulated increase of the overall export production. In their model the global production - 13 Gt C yr^{-1} - was doubled by iron fertilization, where as in our model the global production only increased from 8.5 to 10.7 Gt C yr^{-1}. Both mechanisms in their model tend to produce a subsurface maxium at 60°S which is not seen in our simulations.

Sensitivity to Modifications of the Vertical Structure

The role of the oceanic circulation in reducing the effectivity of the fertilization becomes even clearer from two extreme scenario experiments: We performed one experiment in which all export production in the fertilization area is assumed to reach immediately the nearest to bottom layer of the model. Such a change of the structure of the downward flux could eventually be achieved due to a change in the species composition. The global export production is now limited by lack of nutrient supply. It amounts 8.5 Gt C after 100 years, just incidentally the same number as in the control run. The increase of the penetration depth makes the biological pump more efficient and, thus, increases the effect of fertilization on the atmospheric pCO_2 from 34 ppm to 39 ppm after 100 years.

The second experiment adresses the role of vertical mixing which, in our model, is too strong around Antarctica, as seen by the too

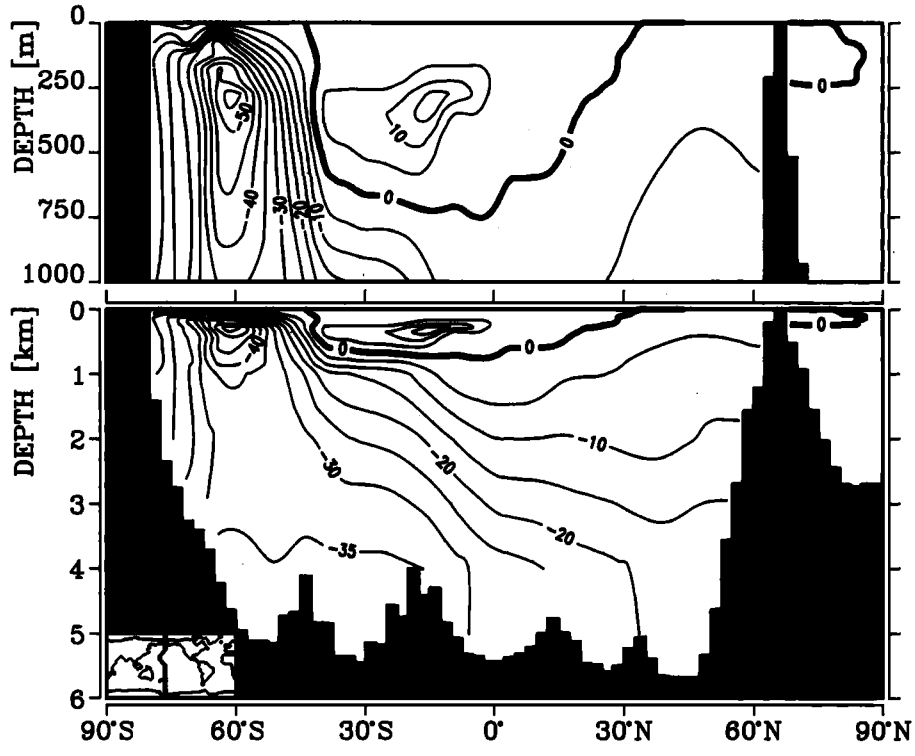

Fig. 7. Change of the oxygen distribution (fertilization - control, in μmol L^{-1}) in the Pacific after 100 years of fertilization. The global average oxygen concentration in the ocean decreases by 4.4 μmol L^{-1}.

high oxygen levels and too young radiocarbon ages in this region. Less mixing would enhance the strength of the biological pump, but it would diminish also the supply of nutrients necessary for the fertilization. We run an experiment in which the mixing provided by convective overturning in regions of deep water formation was switched off. This can be interpreted as a partial switch from the deep transport to the lateral transport case in the Peng and Broecker [1991a, b] model. After 100 years of integration (at which time an atmospheric CO_2 perturbation would be approximately halved), the atmospheric pCO_2 is two ppm less than in the standard run. In this " nonmixing " case, the effect of iron fertilization yields a reduction of approximately 26 ppm after 100 years as compared with the now different reference run. The overestimate of the vertical mixing in the standard run, consequently, introduces an overestimate of the fertilization effectiveness.

Emission Scenarios

The impact of iron fertilization in future is additionally influenced by variations of the effective buffer factor. We performed two experiments with a prescribed anthropogenic emission. The first emission rate was taken from the IPCC scenario A (business-as-usual) [Houghton et al., 1990]. For the second experiment a constant emission rate of 6.35 Gt C was assumed, corresponding to the 1990 emission level including 0.2 Gt C yr^{-1} from the terrestrial biosphere. We started the experiments in the year 1990, after integrating the model from the preindustrial state to 1990 assuming CO_2 emission rates according to Rotty [1981] and Boden et al. [1992]. For both emission scenarios, we performed also a control experiment without fertilization.

The difference between experiment and control run after 100 years is 50 ppm in the business-as-usual case with 1414 Gt C of to-

tal input, and 44 ppm in the constant emission scenario with 635 Gt C. The mean atmospheric pCO_2 reaches values above 850 ppm and 550 ppm, respectively, in the corresponding control scenarios. In the constant emission scenario the fertilization yields a lower absolute number for the atmospheric pCO_2 reduction but a higher percentage of the total input is stored in the ocean.

The difference in the relative effectiveness of the fertilization may be explained be the slowness of the oceanic circulation. The uptake capacity for CO_2 of the deep ocean is limited by the bottleneck of deep-water production regions. A decomposition of the atmospheric CO_2 response to a δ function into a sum of exponentials shows that a substantial fraction of the uptake is characterized by a time constant of several hundred years [Oeschger et al., 1975; Maier-Reimer and Hasselmann, 1987]. The 50 years time constant in the business-as-usual scenario is substantially shorter than this dominant contribution of the oceanic uptake function. For constant small emission from an undisturbed preindustrial state, the airborne fraction would asymptotically be below 20%. In our constant emission control experiment it is accordingly reduced from 67% to 61% after 100 years. The fertilization is now applied in a systems state which is generally more favourable for CO_2 uptake by the ocean. It works like a small effective reduction of the emission and reduces consequently the apparent airborne fraction to 47%. In the high-emission scenario, the effective loss of CO_2 by fertilization is overcompensated by the growth rate of the emission within a very few years.

Compared to the preindustriel experiment - with 34 ppm reduction - the additional uptake of 10 ppm for the constant emission and 16 ppm for the business-as-usual scenario results primarily from the nonlinearity of the buffer factor: For the high-emission scenario it increases from approximately 10 to approximalety 20 [cf. Bacastow, 1981]. Any additional Gt of carbon being taken out from the system by fertilization is, consequently, partitioned to a higher degree from the atmosphere at higher pCO_2 levels. The total air to sea fluxes of CO_2, of course, is favoured by low levels of CO_2.

The results are summarized in Figure 8 which displays the evolution of atmospheric pCO_2 for the four experiments. We chose for the pCO_2 a logarithmic scale according to the dependency of the radiative forcing on CO_2. It is immediately seen that the higher absolute number of pCO_2 reduction by the fertilization in the high-emission scenario involves a smaller impact on the greenhouse potential.

A small additional fixation of carbon could stem from an increased sediment dissolution due to the higher consumption of deep-sea alkalinity in the fertilization experiments. As the acidity of the water rises, shell dissolution releases alkalinity in addition to carbon, which tends to decrease the carbon dioxide partial pressure. In the short simulation period of 100 years, the loss of sediment is less than 3 Gt of carbon and has no noticeable influence on the atmospheric pCO_2.

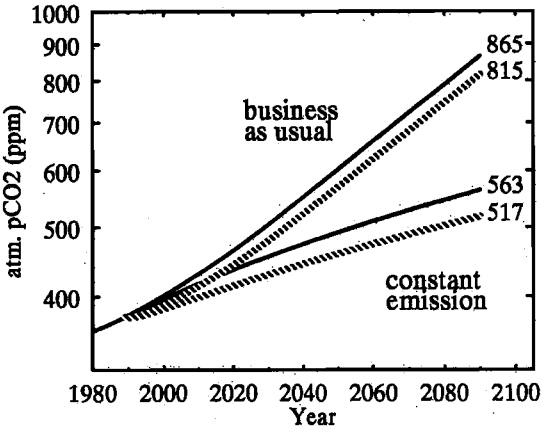

Fig. 8. Time series of the atmospheric CO_2 partial pressure for the business as usual scenario and the constant emission case with fertilization (dashed lines) and the corresponding control scenarios (solid lines). The final concentration (in ppm) are given for each scenario. We used a logarithmic scale for the ordinate according the radiative forcing of CO_2. Note that the difference in the constant emission case is smaller in absolute numbers (44 ppm) but that it has a higher impact on climate.

DISCUSSION

We have shown that the effective removal of atmospheric CO_2 by the iron fertilization is controlled by the time scale in which the organic material is transported back to the surface region. The ocean circulation transports not only nutrients but also carbon to the euphotic zone. We found a time scale of approximately 10 years for half of the organic matter to be brought back to the surface. This explains the difference between our results and those of by Joos et al. [1991] and Peng and Broecker [1991a, b] using box models in which these time constants may be tuned differently. In the Joos et al. model, the organic material of the polar box is released into a well mixed box representative of the deep Antarctic ocean, which exchanges horizontally with the layers of the main deep sea. In addition, a finite fraction enters directly into the base of the global deep upwelling column. The time scale of the reappearance of this carbon is of the order of several hundred years.

Peng and Broecker discussed two different weightings of the governing lateral and deep transports, with pronounced differences in the results. A comparison of the different model results is given in Table 2.

We note that the deep transport version of Peng and Broecker [1991a] assuming a smaller area of fertilization gives the same CO_2 reduction as our model without emissions. The transient behaviour in the case of anthropogenic emissions, however, deviates substantially from our simulation, but the transport parametrization of the Peng and Broecker model is still closer to our three-dimensional model than the parametrization of the Joos et al. model.

A direct comparison with the three-dimensional model by Sarmiento and Orr shows some remarkable similarities of the principal results despite the very different structure of productivity in the basic experiments. The numbers for the effectiveness of the fertilization are slightly higher than our numbers (cf. Table 2). They had started the fertilization south of 30°S, but the additional area of fertilization lies partly in the subtropical gyres of the oceanic circulation with actually very low phosphate concentrations. Since both model use the same data set for wind stress [Hellerman and Rosenstein, 1983], the upwelling and, thus the supply of nutrients are simulated similarly in both models.

CONCLUSIONS

The artificial fertilization of the Austral ocean, even if technically feasible, would do only little to the climatic impact of increasing carbon dioxide. The reduction of atmospheric pCO_2 is highest in a high-emission

TABLE 2. Atmospheric CO_2 Reduction Due to Fertilization of 15 % of World Ocean Area

	This Study	Joos et al.	Peng and Broecker [a]		Sarmiento and Orr
			lateral	deep	
Preindustrial level	34	59	17	34	-
Constant emission	44	90	-	-	61
Business as usual	50	107	64	96	72 (67)[b]

[a] Area of fertilization only 10 % of world ocean.

[b] Number in brackets denotes the model result of Sarmiento and Orr, when they used the same vertical distribution of particular organic matter as in our model.

Comparison between results of the Hamburger carbon cycle model and box model studies [Peng and Broecker, 1991a, b; Joos et al., 1991; Sarmiento and Orr, 1991]. Reduction is in ppm.

scenario. However, the general structure of the ocean circulation together with the nonlinear buffer factor provide a stronger reduction of the airborne fraction at low emissions. Since the radiative forcing varies with the logarithm of the CO_2 concentration, the reduction of the greenhouse potential is additionally more efficient in a low-emission scenario.

We have, in essence, confirmed earlier three-dimensional model studies with a simplified geochemical cycling of the Princeton group who predicted a lower efficiency of the iron fertilization than derived from box models, too.

Acknowledgments. We thank Wallace Broecker and Martin Heimann for helpful discussions and Marion Grunert for preparing the figures. We appreciate the very useful suggestions by James Orr.

REFERENCES

Bacastow, R., and E. Maier-Reimer, Ocean-circulation model of the carbon cycle, *Clim. dyn. 4*, 95-125, 1990.

Bacastow, R., Numerical evaluation of the evasion factor in *Carbon Cycle Modelling*, edited by B. Bolin, pp. 95-101, SCOPE 16, John Wiley, New York, 1981.

Bainbrigde, A. E., *GEOSECS Atlantic Expedition, Hydrographic Data*, vol. 1, National Science Foundation, Washington, D. C., 1981.

Berger, W. H., K. Fischer, C. Lai and G. Wu, Ocean productivity and organic carbon flux, Part I. Overview and maps of primary production and export production, *SIO Ref. 87-30*, Scripps Inst. of Oceanogr., La Jolla, Calif., 1987.

Boden, T. A., R. J. Sepanski, and F.W. Stoss (Eds.), *Trends '91*, Carbon Dioxide Information Analysis Center, Oak Ridge National Laboratory, Oak Ridge, Tenn., 1992.

Broecker, W. S., and T. H. Peng (Eds.), *Tracers in the Sea*, 690 pp., Eldigio, Palisades, New York, 1982.

Broecker, W. S., T. H. Peng, G. Östlund, and M. Stuiver, The distribution of bomb radiocarbon in the ocean, *J. Geophys. Res., 90*, 6953-6870, 1985.

Davies, A., Taking a cool look at iron, *Nature, 345*, 114-115, 1990.

Eppley, R. W., J. N. Rogers, and J. J. McCarthy, Half-saturation constants for uptake of nitrate and ammonium by marine phytoplankton, *Limnol.Oceanogr., 14*, 912-920, 1969.

Heimann, M., and P. Monfray, Spatial and temporal variation of the gas exchange coefficient for CO_2, 1, Data analysis and global validation, *MPI Rep. 31*, Max-Planck-Inst. für Meteorol., Hamburg, Germany, 1989.

Heinze, C., E. Maier-Reimer, and K. Winn, Glacial pCO_2 reduction by the world ocean: Experiments with the Hamburg carbon cycle model, *Paleoceanogr., 6*, 395-430, 1991.

Hellerman, S., and M. Rosenstein, Normal monthly wind stress over the world ocean with error estimates. *J. Phys. Oceanogr. 13*, 1093-1104, 1983.

Houghton, J.T., G.J. Jenkins, and J.J. Ephraums (Eds.), *Climate Change: The IPCC Scientific Assessment*, Cambridge University Press, New York, 1990.

Joos, F., J. L. Sarmiento, and U. Siegenthaler, Estimates of the effect of Southern Ocean iron fertilization on atmospheric CO_2 concentrations, *Nature, 349*, 772-775, 1991.

Levitus, S. (Ed.), *Climatological Atlas of the World Ocean*, NOAA Prof. Pap. 13, U.S. Government Printing Office, Washington, D. C., 1982

Liss, P. S., and L. Merlivat, Air-sea gas exchange rates: introduction and synthesis, in *The Role of Air-Sea Exchange in Geochemical Cycling*, edited by P. Buat-Ménard, pp. 113-127, D. Reidel, Hingham, Mass., 1986.

Maier-Reimer, E., and R. Bacastow, Modelling of geochemical tracers in the Ocean, in *Climate-Ocean Interaction*, vol. C243 *NATO ASI Ser.*, edited by M. E. Schlesinger, pp. 233-267, Kluwer Academic, Boston, Mass., 1990.

Maier-Reimer, E., and K. Hasselmann,

Transport and storage of CO_2 in the ocean - An inorganic ocean-circulation carbon cycle model, *Clim. Dyn. 2*, 63-90, 1987.

Maier-Reimer, E., U. Mikolajewicz, and K. Hasselmann, Mean circulation of the Hamburg LSG OGCM and its sensitivity to the thermohaline surface forcing, *J. Phys. Oceanogr.*, in press, 1993.

Martin, J. H., R. M. Gordon, and S. E. Fitzwater, Iron in Antarctic waters, *Nature, 345*, 156-158, 1990.

Najjar, R. G., J. L. Sarmiento, and J. R. Toggweiler, Downward transport and fate of organic matter in the ocean: Simulations with a general circulation model, *Global Biogeochem. Cycles, 6*, 45-76 , 1992.

Oeschger, H., U. Siegenthaler, U. Schotterer, and A. Gugelmann, A box diffusion model to study the carbon dioxide exchange in nature, *Tellus, 27*, 168-192, 1975.

Peng, T. H., and W. S. Broecker, Dynamical limitations on the Antarctic iron fertilization strategy, *Nature, 349*, 227-229, 1991a.

Peng, T. H., and W. S. Broecker, Factors limiting the reduction of atmospheric CO_2 by iron fertilization, *Limnol. Oceanogr., 36*(8), 1919-1927, 1991b.

Peng, T. H., W. S. Broecker, H. D. Freyer, and S. Trumbore, A deconvolution of the tree rings based $\delta^{13}C$ record, *J. Geopys. Res. 89*, 3609-3620, 1983.

Rotty, R. M., Data for global CO_2 production from fossil fuel and cement, in *Carbon Cycle Modelling*, SCOPE 16, edited by B. Bolin, 121-127, John Wiley and Sons, New York, 1981.

Sarmiento, J. L., and J. C. Orr, Three-dimensional simulations of the impact of Southern Ocean nutirent depletion on atmospheric CO_2 and ocean chemistry, *Limnol. Oceanogr., 36*(8), 1928-1950, 1991.

Sarmiento, J. L., J. C. Orr, and U. Siegenthaler, A perturbation simulation of CO_2 uptake in an ocean general circulation model, *J. Geophys. Res., 97*(C3), 3621-3645, 1992.

Siegenthaler, U., Uptake of excess CO_2 by an outcrop-diffusion model of the ocean, *J. Geophys. Res., 88*, 3599-3608, 1983.

Siegenthaler, U., and H. Oeschger, Biosheric CO_2 emission during the past 200 years reconstructed by deconvolution of ice core data, *Tellus, Ser. B 39*, 140-154, 1987.

Stuiver, M., and H.G. Östlund, GEOSECS Atlantic radiocarbon, *Radiocarbon 22*, 1-24, 1980.

Suess, E., Particulate organic carbon flux in the oceans - Surface productivity and oxygen utilization, *Nature, 288*, 260-263, 1980.

Tans, P. P., I. Y. Fung, and T. Takahashi, Observational constraints on the global atmospheric CO_2 budget, *Science, 247*, 1431-1438, 1990.

Whitfield, M., Do we understand the carbon cycle ?, paper presented at the First Demetra Meeting on Global Change, Demetra Society, Chianciano Therme, Italy, Oct. 28 to Nov. 1 , 1991.

Woodruff, S. D., R. J. Slutz, R. L. Jenne, and P. M. Steurer, A comprehensive ocean-atmosphere data set, *Bull. Am. Soc., 68*, 1239-1250, 1987.

K. D. Kurz and E. Maier-Reimer, Max-Planck-Institut für Meteorologie, Bundesstrass 55, D-2000 Hamburg 13, Germany.

(Received May 29, 1992;
revised December 3, 1992;
accepted December 10, 1992.)